Radiation Parameterization for Climate Models: Some New Perspectives (invited paper presented at the AGU Fall meeting, San Francisco, December 14, 2010)

First, I would like to thank Yangang Liu and Leo Donner for inviting me to present a paper on the subject of radiation parameterization for climate models. To provide a background for my talk, I will first introduce the atmospheric composition and solar and thermal infrared radiation spectra, followed by a note on the evolution of radiation parameterization in GCMs, using the UCLA GCM as a prototype. Subsequently, I will discuss a number of unsolved problems in radiative transfer, and focus on two contemporary subjects: Mountains/snow and absorbing aerosols.

This Slide (2) depicts the atmospheric composition, including absorbing gases, Rayleigh molecules, aerosols, clouds, precipitation, and surface features, which must be effectively accounted for in radiation parameterization on the basis of the first principle for use in climate models.

The following Slide (3) shows the solar and thermal IR radiation spectra. In these two diagrams, the principal absorbing gases are identified. The IR spectrum was obtained from the Scanning High-Resolution Interferometer Sounder with a spectral range from 3.3 to 18 □m.

The next Slide (4) presents the evolution of radiation treatment in the UCLA GCMs, beginning with the Mintz-Arakawa Model developed in 1963, which used an empirical approach to determine solar and IR heating rates to drive the model. The second-generation GCM developed in 1972 included the calculations of broadband IR fluxes and cooling rates determined from Yamamoto's radiation chart. Katayama also developed a geometric-tracing technique to obtain cloud albedo. Later, Mike Schlesinger added solar absorption produced by ozone to the GCM. Subjects of cumulus parameterization and PBL depth became the main focus of model developments in the 70s and 80s. It was not until the mid 90s that a broadband radiation scheme developed by Harshvardham was incorporated into the UCLA Generation 5 GCM. Martin Kohler developed prognostic ice and water content equations for the model as a part of his Ph.D. dissertation in 1999. At about the same time, Yu Gu and I incorporated the Fu-Liou radiation scheme into the UCLA AGCM. We did so with the help of John Farrara and Roberto Mechoso and we published in 2003 our first GCM paper with a spectral radiation parameterization including all the greenhouse gases, interactive cloud cover formation scheme, and ice cloud optical properties.

This Slide (5) illustrates the current Fu-Liou-Gu radiation parameterization, which contains two unique features: First, the coupling of the correlated k-distribution for sorting absorption lines and the

delta-4-stream approximation for radiative transfer. As shown in Fu and Liou (1992, 1993), this parameterization produces accuracies in radiative fluxes within about 5%, as compared with the "exact" line-by-line and adding/doubling radiative transfer calculations. Secondly, we provided an innovative parameterization of the single-scattering properties of ice crystals based on theoretical scattering and absorption calculations for nonspherical and irregular ice particles, as well as observed size and shape distributions.

The next Slide (6) demonstrates that the incorporation of our radiation scheme, as compared to that of Harshvardham, alleviates the cold bias in the model associated with greater solar absorption in the atmosphere and the surface, and traps more IR radiation at the surface. As a result, the Fu-Liou-Gu radiation parameterization produced substantial improvements in zonal mean temperature simulations in both January and July, as compared with observations.

Slide 7: In parameterization of the single-scattering properties of ice crystals, we developed a number of linear Polynomial equations for the extinction coefficient, single-scattering albedo, and four expansion coefficients in phase function, based on observed size and shape distributions and the scattering and absorption data compiled by Yang et al. (1999, 2005). Our extinction coefficients and phase functions for ice particles compared reasonably well with nephelometer results obtained from our lab ice cloud chamber. On the basis of thermodynamic principles, we have also derived a parameterization to correlate the ice water content, which is a prognostic variable in GCMs, with a mean effective ice crystal size, generally assumed a constant value, to drive radiative transfer calculations.

Slide 8: We used the observed ice crystal size and shape distributions derived from a number of field experiments sponsored by ASR/DOE programs, classified them into three groups according to regions, and accounted for uncertainties in small ice crystals due to shattering effects. We then developed a number of linear correlation equations for IWC and De, which can be directly used for radiative forcing and climate perturbation studies. The parameterization equations provide a means to obtain ice crystal size that cannot otherwise be determined from the current GCMs for radiation calculations involving ice clouds. In the panel on the right, we demonstrate via the UCLA AGCM substantial differences in the regional context in simulated OLR and precipitation patterns between interactive and fixed ice crystal sizes. This analysis also illustrates the usefulness of ASR/DOE observed ice cloud datasets associated with the development of physically-based parameterization for direct application to climate models for interaction and process studies involving ice clouds and

aerosols.

In the next Slide (9), I have identified a number of unsolved problems in radiative transfer in conjunction with climate research. These include (1) radiative transfer in ice crystal clouds, which in my opinion has been largely resolved, although several issues remain outstanding; (2) radiative transfer in the atmosphere and ocean system involving inhomogeneous and 3D ocean surfaces generated by surface winds. Also, the absorption of sunlight by phytoplankton is important in the ocean mixed layer; (3) radiative transfer in 3D mountains/snow; and (4) radiative transfer in absorbing aerosols. I shall focus on the last two and I would submit that they are critically important in building a physically-based and reliable regional climate model.

Slide 10: This slide presents a number of snow scenes over the Sierra-Nevada and Rocky Mountains in the United States, the Alps in Europe, and the Tibetan Plateau in China. Mountains and snow are common topographical features. They are 3D in nature and cannot be treated as flat surfaces to which the conventional plane-parallel radiative transfer program can be applied.

Slide 11: It appears unlikely that analytical solutions, such as 2-stream, Eddington, and 4-stream approximations for radiative transfer, can be derived for intricate mountains/snow fields. In my opinion, the only solution is by means of the Monte Carlo simulation, which can be applied to any geometry, but unfortunately, formidable computational efforts are required to achieve reliable accuracy. We have made significant advances in modeling the transfer of solar and thermal IR radiation involving intense topography following Monte Carlo photon tracing. The transfer of solar radiation is composed of 5 components- direct, diffuse, direct-reflected, diffuse-reflected, and coupled fluxes- related to the solar incident angle, elevation, sky view factor, and terrain configuration factor.

The following Slide (12) illustrates differences between the domain-averaged net radiative flux on mountains and a flat surface as a function of the time of day using two domains of 30 and 50 km (centered at Lhasa, Tibet) on March 21 (equinox). In reference to a flat surface, 3D mountain effects can produce about 10-30 W/m^2 differences in solar fluxes in a regional scale of 30 km domains. Longwave radiation only shows differences less than 5 W/m^2. The radiation flux component of 10-30 W/m^2 is indeed substantial and must be accounted for in the evaluation of surface temperature perturbation, especially over snow surfaces.

This Slide (13) displays a comparison of the deviations (from plane-parallel results) of the five flux components computed from Monte Carlo simulations (real values) and multiple regression equations (predicted values) using a domain of 10 km. The upper panel is for direct and diffuse fluxes. The

middle panel is for direct-reflected and diffuse-reflected fluxes. The lower panel shows the coupled flux with a surface albedo of 0.1 and 0.7. The most important component is direct flux (~ 700 W/m^2), followed by direct-reflected flux. We have derived 5 universal regression equations for flux deviations which have the general linear form for the 5 flux components, as shown in the lower panel. For example, for the deviation of direct flux, F^*_{dir}, we have $a_1 + b_{11}\, y_1 + b_{12}\, y_2$, where y_1 is the mean cosine of the solar zenith angle, y_2 is the mean sky view factor, and b_{11} and b_{12} are regression coefficients. This parameterization is applicable to clear as well as cloudy conditions using cloud optical depth as a scaling factor. The flux deviation results can be directly added to the existing surface flux values determined from a land-surface model to account for 3D mountain effects.

Slide 14: I shall now confine my presentation to radiative transfer in aerosols and focus on black carbon. Soot or BC particles are complex with regards to their size, morphology, and composition. They are aggregations of individual monomers, which can be structured in terms of internal and external mixing resulting in open and closed clusters, leading to substantial differences in their absorption and scattering properties, critically important in climate study. We have recently developed a new theoretical approach, which combines a stochastic process to build aggregates, followed by the geometric photon tracing including reflection/refraction, diffraction, and surface waves. The building block can be homogeneous or coated spheres with smooth or rough surfaces. We show an example of the stochastic process to construct aggregates that resemble observed shape in the air. The light absorption and scattering program by small irregular particles based on the geometric-optics and surface-wave approach has been verified by comparison with existing results for columns and plates.

This Slide (15) depicts the extinction efficiency, single-scattering albedo, asymmetry factor, and specific absorption as a function of a volume equivalent size parameter. 256 spheres were used to build BA and DLA based on stochastic procedures. Each building sphere in a closed cell contains 90% soot core and 10% nonabsorbing sulfate shell. In an open cell, 70% are soot and 30% are sulfate such that volume and mass are the same in all cases in order to have a physically-based comparison. We show that closed cell cases have larger absorption and stronger forward scattering, as compared to open cell counterparts. Also, DLA absorbs more than BA because of larger geometrical cross section.

In the following Slide (16), we illustrate the importance of the contamination of snow grains by absorbing aerosols. Internal mixing produces much larger absorption, as compared with its external counterpart, in terms of a larger single-scattering co-albedo. The subsequent radiative transfer calculations illustrate reduction of snow albedo associated with the contamination of BC and dust

particles, depending on their size. Due to its larger absorption, BC has a more substantial impact than dust particles on reducing snow albedo.

This Slide (17) demonstrates the essence of mountains/snow-albedo feedback, a powerful amplification process involving absorbing aerosols. Through the wet and/or dry deposition of absorbing aerosols, snow becomes less bright. As a consequence, it will absorb more incoming sunlight, which will lead to surface warming. The loop involving darker snow and greater sunlight absorption forms a powerful feedback that can significantly amplify increase in surface temperature.

In summary (Slide 18): (1) We have identified a number of important and unsolved problems in radiative transfer and the needs for parameterization based on the first principle for climate models. (2) Over a domain of 10-30 km resolution, the 3D effects on intense topography can produce about 10-30 W/m^2 deviations from plane-parallel radiative transfer calculations commonly used in land surface models. We have illustrated that a regression-based parameterization for 3D direct, diffuse and interactive solar fluxes is ready for testing in WRF-Community Land-surface model developed by Ruby Leung. (3) Finally, we have made fundamental advances in light absorption and scattering by aggregates (black carbon), but we need to comprehend the observed size, shape, and composition data to develop a useful parameterization for regional air-quality and climate models.

Radiation Parameterization for Climate Models: Some New Perspectives

[1]K. N. Liou, [1]Y. Gu, [2]W. L. Lee, [1]Y. Takano
[1]Joint Institute for Regional Earth System Science and Engineering (JIFRESSE) and Atmospheric and Oceanic Sciences Department
University of California, Los Angeles, CA, USA
[2]Academia Sinica, Taipei, Taiwan

- Atmospheric Compositions; Solar and Thermal IR Radiation Spectra
- UCLA GCM Radiation Parameterization: Past and Present
- Some Unsolved Problems in Radiative Transfer
- Radiative Transfer in Mountains/Snow: Snow-Albedo Feedback
- Radiative Transfer in Aerosols: Black Carbon and Dust
- Summary

Radiation Parameterization for Climate Models

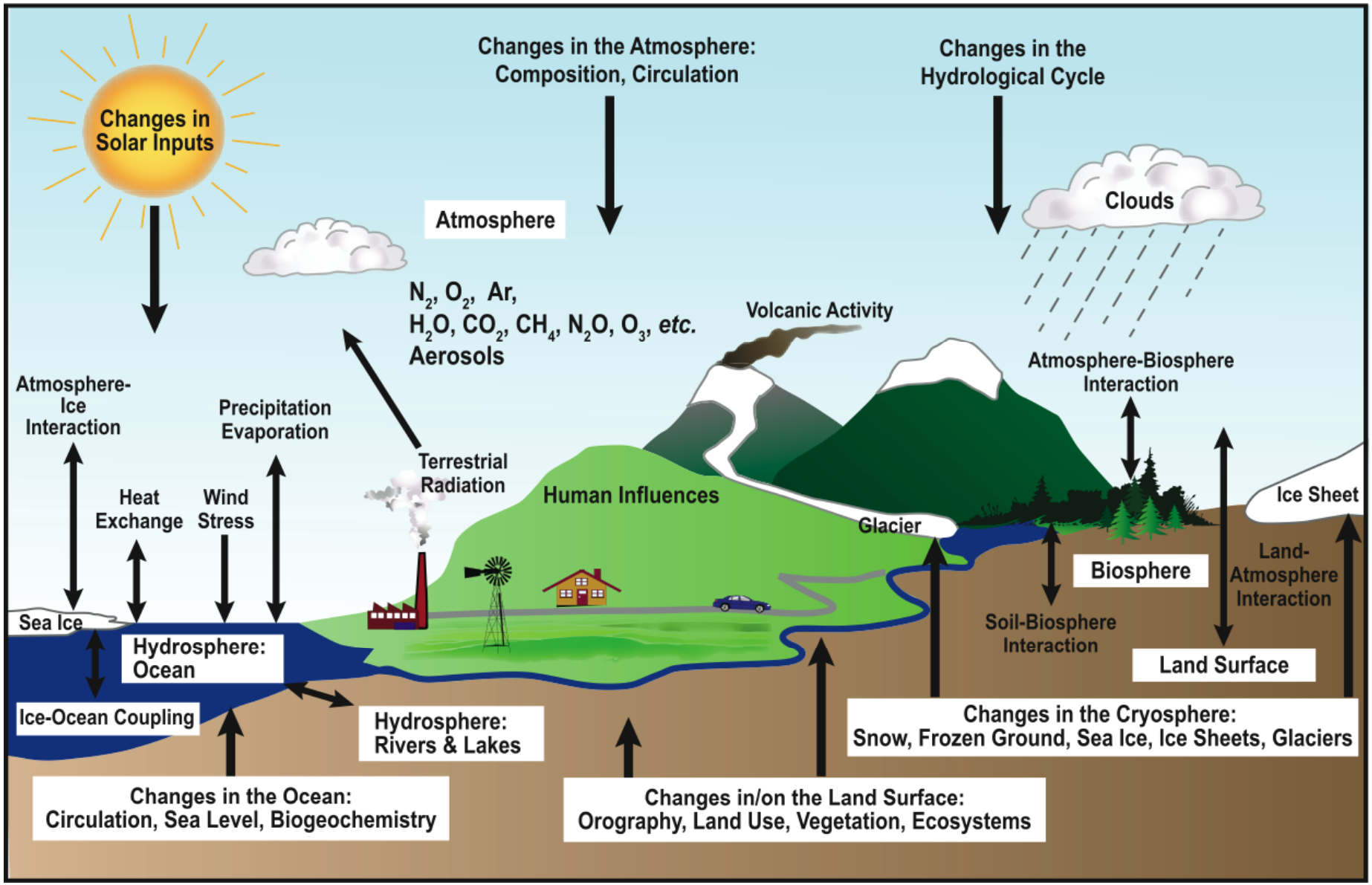

A schematic view of the components of the climate system, their processes and interactions (IPCC)

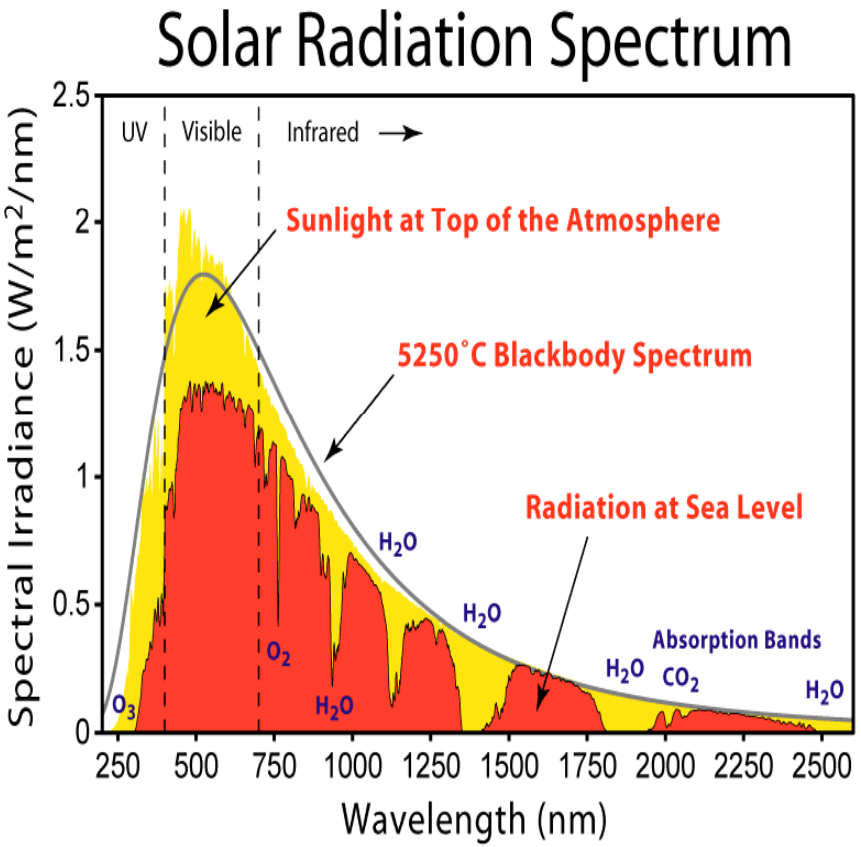

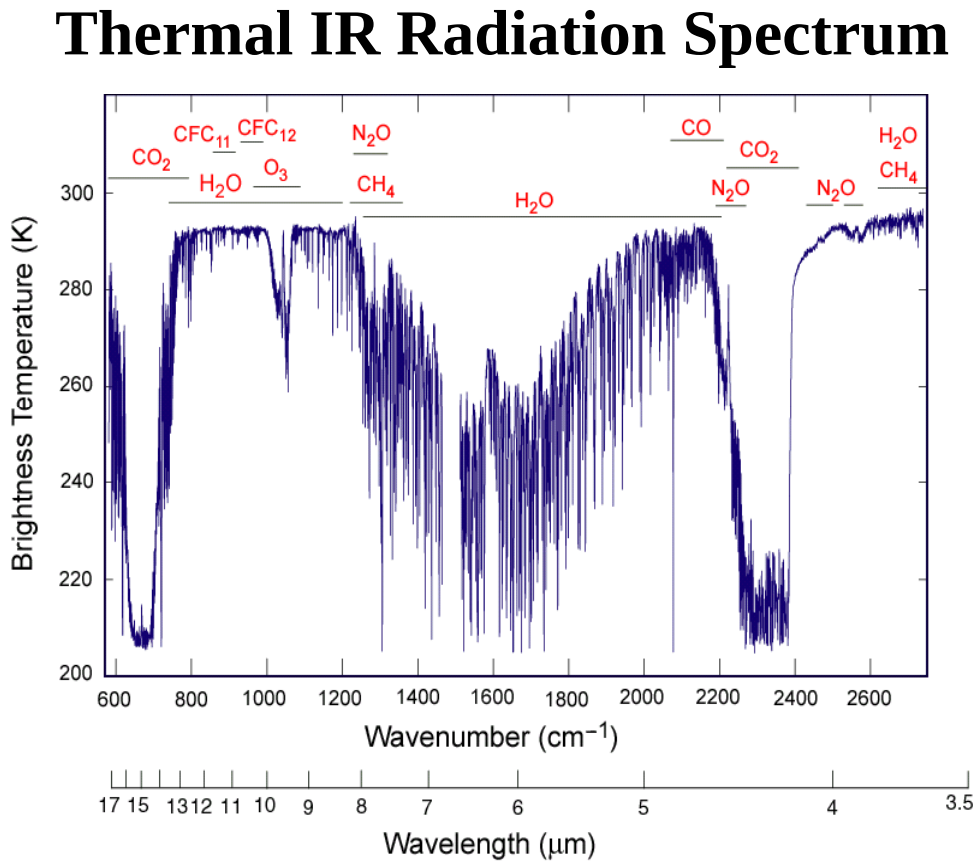

Observed solar and thermal infrared spectra displaying principal absorbing gases and their spectral location. The IR spectrum was obtained from the Scanning High-resolution Interferometer Sounder (S-HIS), which measured the emitted thermal radiation between 3.3 and 18 μm, onboard the NASA ER-2 aircraft over the Gulf of Mexico southeast of Louisiana, on April 1, 2001 (courtesy of Allen Huang and Dave Tobin of the University of Wisconsin).

A Note on Radiation Parameterization in the UCLA GCM*

- **Mintz-Arakawa Model (Generation I GCM, 2-level, 1963): Included seasonal changes of solar radiation. Longwave cooling for each layer was empirically determined (Takahashi et al. 1960).**
- **Generation II GCM (2-level, 1972): Explicit calculation of radiative transfer using the schemes developed by Katayama (1969, 1982) and Schlesinger (1976).**
- **Generation III GCM (12-level, 1977): Inclusion of the Arakawa-Schubert cumulus parameterization (Arakawa 1972; Schubert 1973; Arakawa and Schubert 1974). No change in radiation scheme.**
- **Generation IV GCM (15-level, 1983): Inclusion of a variable-depth PBL (Suarez et al 1983). No change in radiation schedule.**
- **Generation V GCM (15-level, 1997): Explicit calculation of radiative transfer using the scheme developed by Harshvardhan et al. (1987). Prognostic liquid water and ice (Kohler 1999).**
- **Recent Versions: Radiation parameterization improvements in 6.62, 6.63, 6.9, 7.0, 7.3 and others (Gu et al. 2003, based on Fu and Liou 1992, 1993).**

*** We thank A. Arakawa and C. R. Mechoso for their helpful comments.**

Radiation Parameterization for Climate Models: Fu-Liou-Gu Scheme Specifically Designed for Clouds (Ice) and Aerosols

- **Gaseous absorption: Correlated k-distribution method (Fu and Liou 1992; Zhang et al. 2005). Solar absorption: H_2O and continuum, O_3, CO_2, O_2, CO, CH_4, N_2O, NO_2, O_2-O_2, and O_2-N_2; Thermal IR absorption: H_2O and continuum, O_3, CO_2, CH_4, N_2O, and CFCs; Rayleigh Scattering.**
- **Radiative Transfer: Delta-4 stream approximation for solar radiation (Liou 1974; Liou et al. 1988) and combined delta-2/4 stream approximation for thermal IR radiation (Fu et al. 1997): Application of the similarity principle to each grid point to account for strong diffraction of aerosol and cloud particles.**
- **Spectral Bands: Six bands for solar (0-5 μm) and 12 bands for IR (5-50 μm); 121 spectral calculations for each vertical profile (Fu and Liou 1992; 1993).**
- **Single-scattering Properties of Ice Particles: Parameterized in terms of the observed size and shape spectra (Fu and Liou 1993; Yang et al. 1999 (Sol), 2005 (IR); Liou et al. 2008).**
- **Mean effective ice crystal size: parameterized in terms of IWC to represent ice crystal size distribution in radiative transfer calculations (Liou et al. 2008).**
- **Single-scattering Properties of Aerosols: Parameterized 18 aerosol types for 60 wavelengths in the spectral region between 0.3 μm and 40 μm; interpolated into the Fu-Liou-Gu spectral bands; vertically distributed and dependent upon aerosol type and relative humidity (Gu et al. 2006; Gu et al. 2010).**

Zonal Mean Temperature

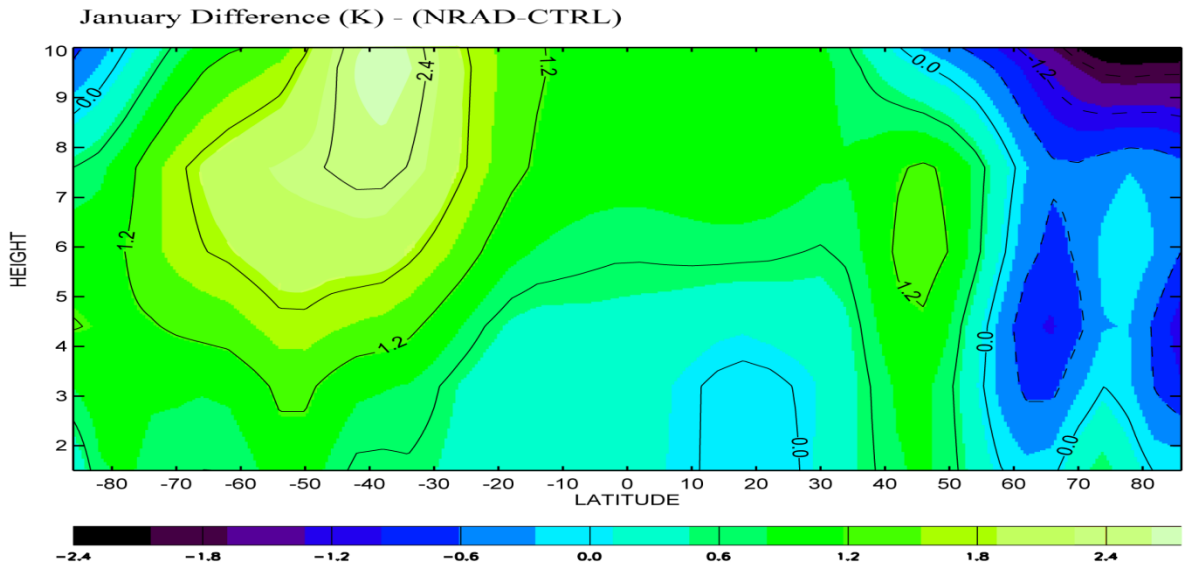

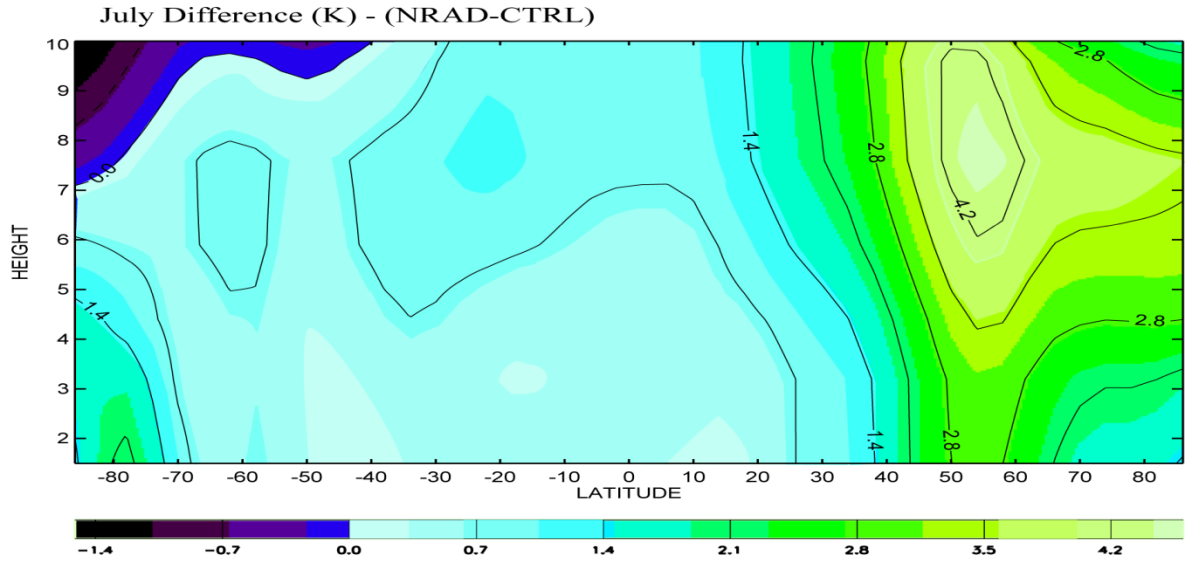

Total differences in radiative fluxes in the UCLA AGCM (Fu/Liou/Gu – Harshvardhan)

	Solar	Net	IR
	+6.07 ⇓	+6.34 ⇓	+0.27 ⇓
TOA			
	+1.67 ⇓	+2.94 ⇓	+1.27 ⇓
SFC			

Note: The Fu-Liou-Gu radiation scheme provides for greater absorption of solar and IR radiative fluxes in the atmosphere and the surface than those computed from the Harshvardhan scheme, alleviates model cold bias, and improves zonal mean temperature simulations in January and July (Gu et al. 2003).

Light Scattering and Absorption Parameterization for Ice Crystals (Fu and Liou 1993; Gu et al. 2003, 2006)

- **Extinction Coefficient**

$$\beta_e = IWC\,(a_0 + a_1/D_e + a_2/D_e^2)$$

- **Single-Scattering Co-albedo**

$$1 - \varpi_0 = b_0 + b_1 D_e + b_2 D_e^2$$

- **Asymmetry Factor**

$$g = c_0 + c_1 D_e + c_2 D_e^2 \text{ (also } \varpi_2, \varpi_3, \text{ and } \varpi_4)$$

- $N \approx 2$ (IR, 12 bands); $N \approx 1$ (SOL, 6 bands, $Q_e \rightarrow 2$)
- a_n, b_n, and c_n: fitting coefficients determined from light scattering data (Yang et al. 1999, SOL; Yang et al. 2005, IR)
- Shape factor: 50% bullet rosette/aggregate; 30% hollow column; 20% plate

Radiative Transfer: Ice Crystal Size Parameterization (Liou et al. 2008)

- Ice Water Content (a prognostic variable in GCMs)

$$IWC = \int V \rho_i n(L) dL$$

- Ice Crystal Size Distribution (unknown in GCMs)

$$n(L)\ [(L_{min}, L_{max});\ \textit{shape factor}]$$

- Mean Effective Ice Crystal Size (for radiation calculations)

$$D_e = \int V n(L) dL \,/\, \int A n(L) dL = IWC \,/\, \rho_i A_t$$

V=volume, A=effective cross section, ρ_i=ice density, and L=length

Application of ARM/DOE Ice Cloud Data to GCMs and Climate Models (Liou et al. 2008)

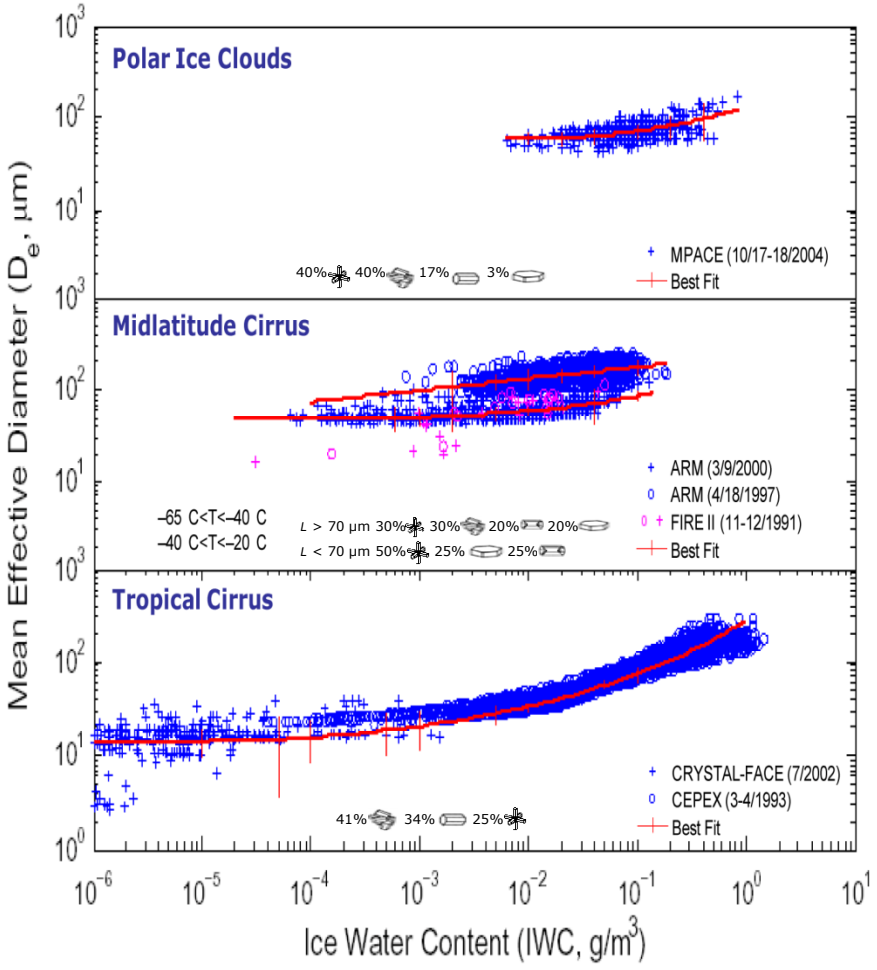

Fig. 1. Mean correlation curves with uncertainties associated with small ice crystal concentration (vertical bars) for IWC and D_e (ice crystal size) : Tropics (bottom), Midlatitude (middle, with a temperature classification), and Arctic (top).

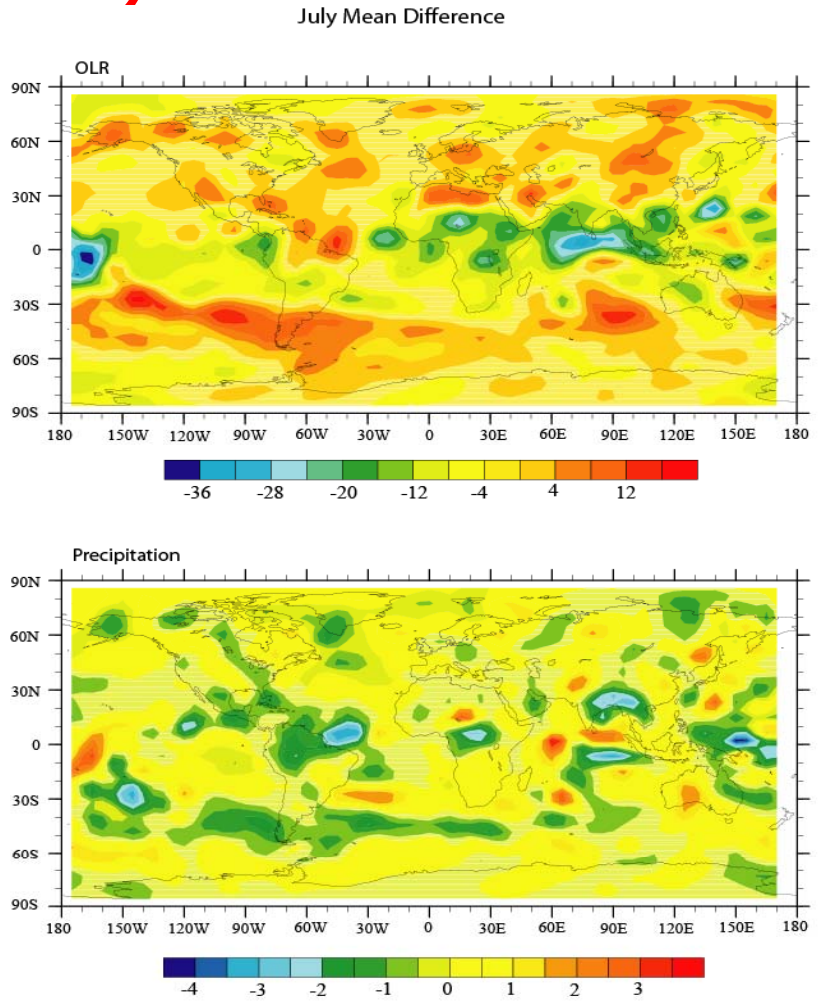

Fig. 2. July mean Differences in the OLR (W/m^2, top) and precipitation (mm/day, bottom) patterns between UCLA GCM simulations based on D_es determined from the IWC-D_e correlations and the control run using a fixed ice crystal size (80 μm).

Some Unsolved Problems in Radiative Transfer and Climate Research

- **Radiative Transfer in Ice Crystal Clouds (Almost Resolved; Contrails and Contrail-Cirrus; Small Ice crystals): Cirrus-Aerosol Interaction, Cirrus-Water Vapor in the Tropic, Radiative Forcing**
- **Radiative Transfer in the Atmosphere-Ocean System: Surface Winds (3D) and Phytoplankton**
- **Radiative Transfer (3D) in Mountains/Snow (Snow-Albedo Feedback): Some New Perspectives**
- **Radiative Transfer in Aerosols (Black Carbon and Dust): Some New Perspectives**


Sierra Nevada (America)


Rocky (America)

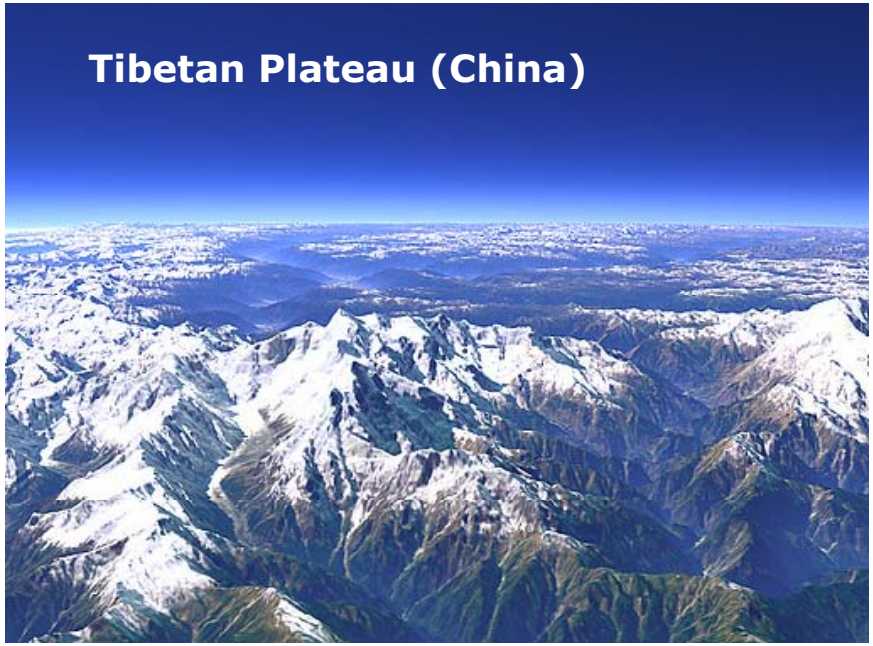
Tibetan Plateau (China)


Alps (Europe)

3D Radiative Transfer (Monte Carlo Photon Tracing) in Mountains: 10-30 W/m² in Regional Surface Energy Balance (Liou et al. 2007; Lee et al. 2010, regression parameterization for use in WRF-CLM)

Solar radiation:

- Direct: solar incident angle θ_i
- Diffuse: sky view factor V_d
- Direct reflected: terrain configuration factor C_t
- Diffuse reflected: terrain configuration factor C_t
- Coupled: terrain configuration factor C_t

Thermal infrared radiation:

- Emitted in the atmosphere or from the surface
- Starting location sampled from a set of pre-divided cubic cells
- Random direction and isotropic emission (emissivity & temperature)

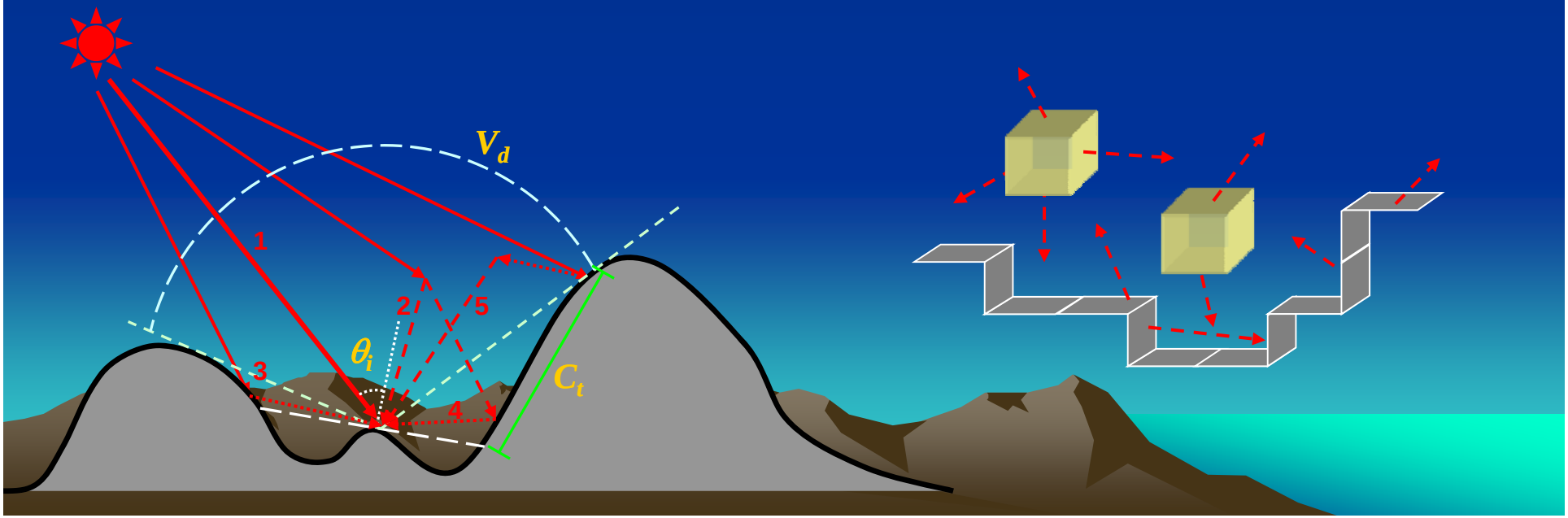

Differential Equation for Land Surface Temperature

$$C_{ps}\, dT_s/dt = F_S + F_{IR} + F_H + F_{IS}$$

where C_{ps} is the surface heat capacity; t is time; F_s, F_{IR}, and F_H represent net solar, long-wave, and heat fluxes at the surface, respectively; F_{IS} denotes fluxes associated with ice/snow melting. With reference to a flat surface, **3D mountain effects can produce 10-30 W/m^2 differences in solar fluxes in 30x30 km^2 domains.**

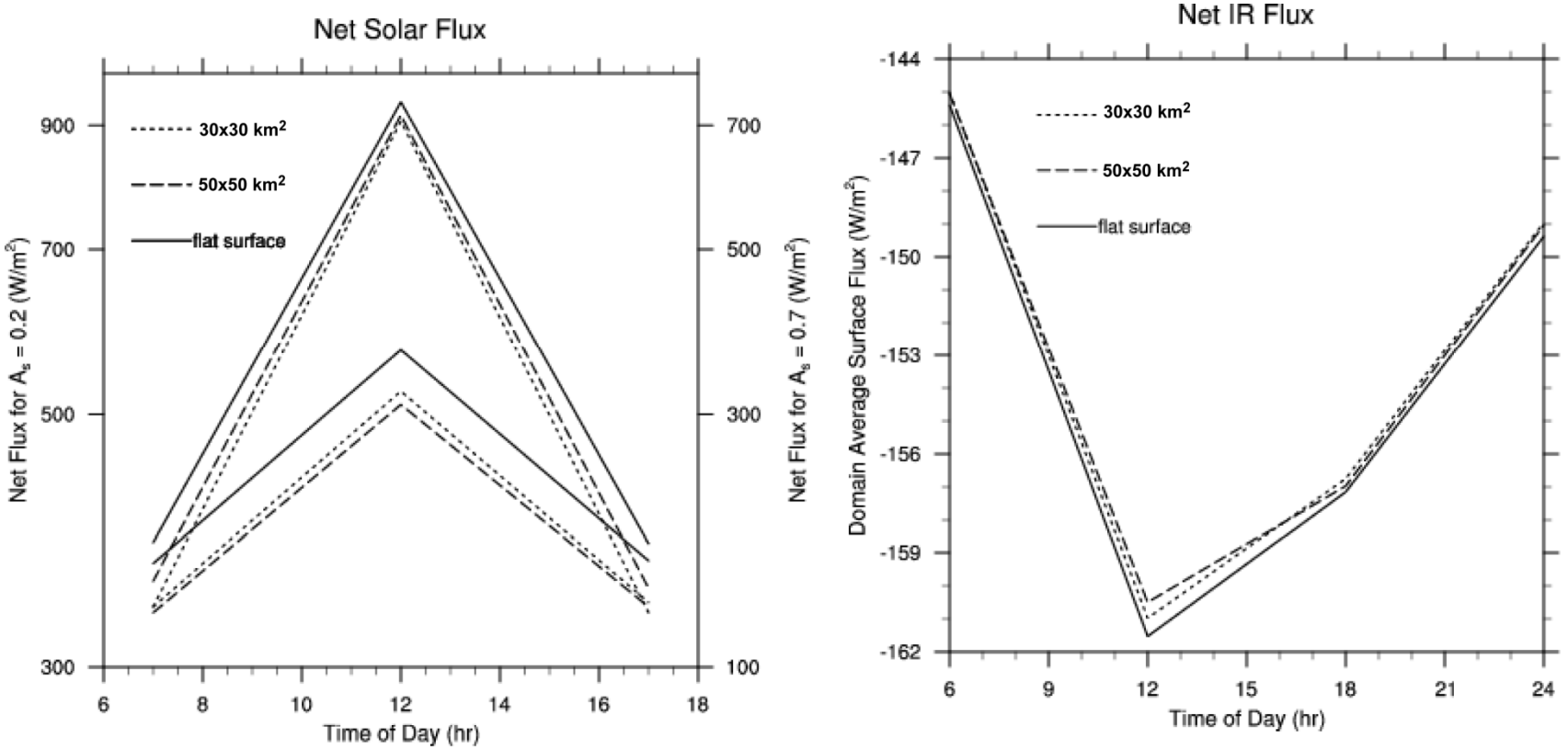

Differences between the domain-averaged net radiative flux on mountains and a flat surface as a function of time of day using surface albedo values of 0.2 and 0.7 for two domains of 30×30 km^2 (centered at Lhasa, Tibet) and 50×50 km^2 on March 21 (equinox).

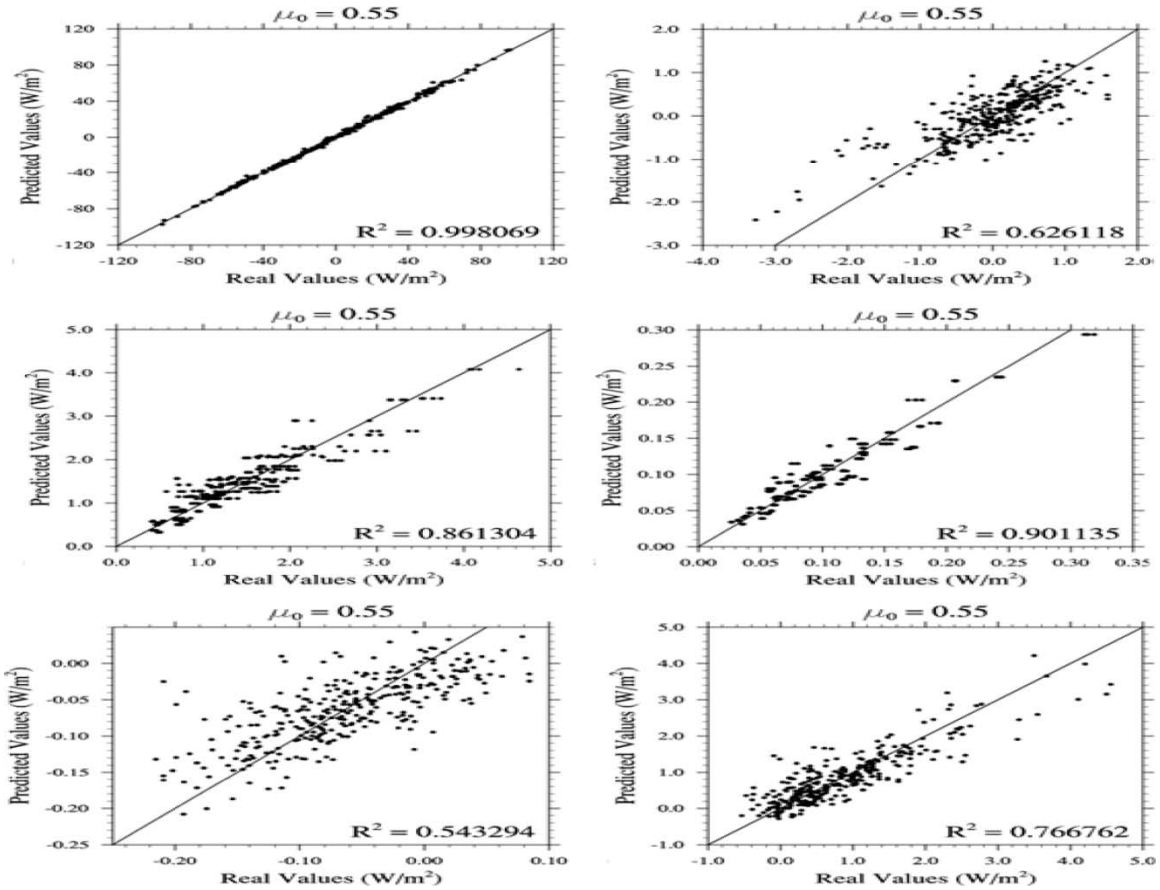

Comparison of the deviations of the five flux components computed from Monte Carlo simulations (real values) and multiple regression equations (predicted values). The upper panel is for direct (left) and diffuse (right) fluxes. The middle panel is for direct-reflected (left) and diffuse-reflected (right) fluxes. The lower panel shows the coupled flux with a surface albedo of 0.1 (left) and 0.7 (right). The most important component is direct flux (~ 700 W/m^2), followed by direct-reflected flux (Lee et al. 2010).

We have derived 5 universal regression equations for flux deviations which have the following general form:

$$F^*_i = a_i + \Sigma\, b_{ij}\, y_j,\ i = \text{dir, dif, dir-ref, dif-ref, and coup,}$$

where a_i is the intercept, y_j is a specific variable, and b_{ij} are regression coefficients. For example, for the deviation of direct flux, we have $F^*_{dir} = a_1 + b_{11}\, y_1 + b_{12}\, y_2$, where y_1 is the mean cosine of the solar zenith angle and y_2 is the mean sky view factor. This parameterization is applicable to clear as well as cloudy conditions using cloud optical depth as a scaling factor.

Construction of aggregates based on stochastic processes using homogeneous and shell spheres (smooth and irregular) as building blocks (Liou et al. 2010): closed and open cells, and observed soot

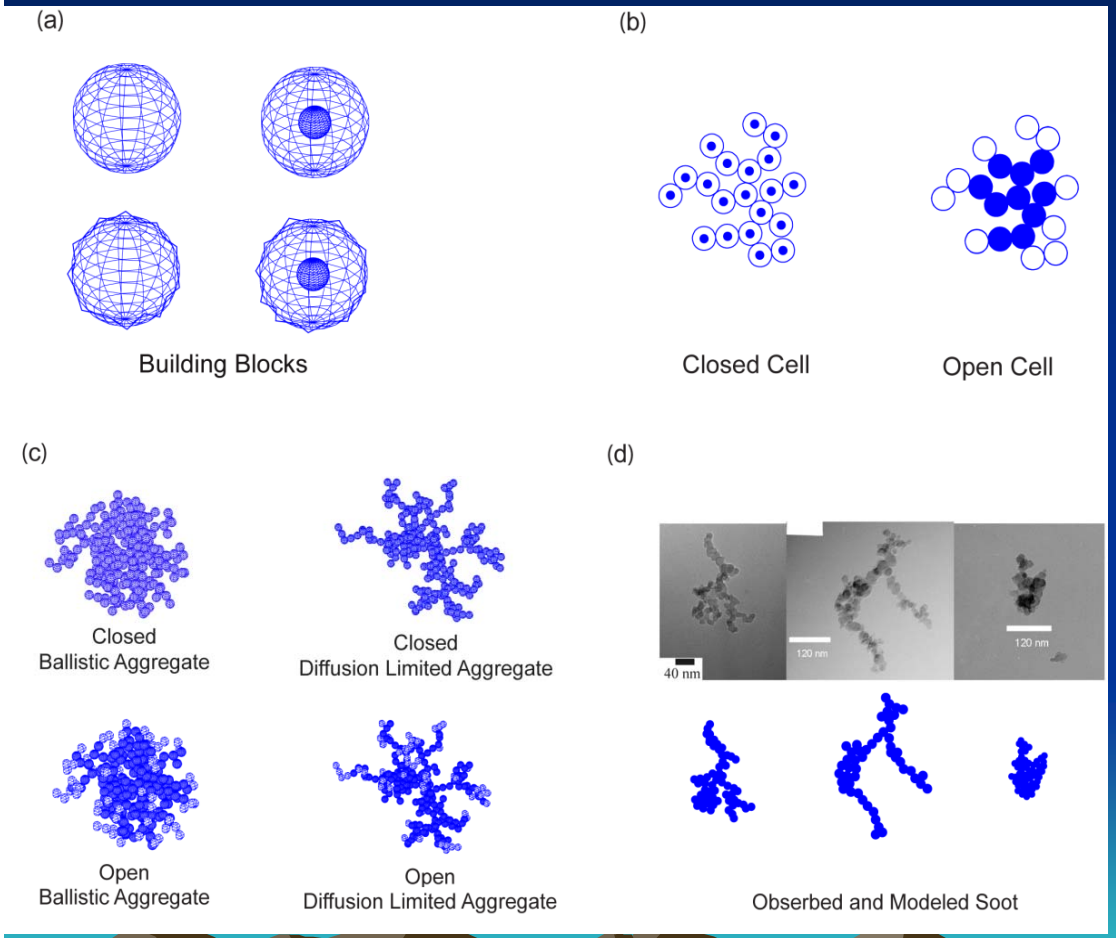

Light absorption and scattering by small irregular particles based on the geometric-optics and surface-wave approach verified by comparison with existing results for columns and plates (Liou, Takano and Yang 2010)

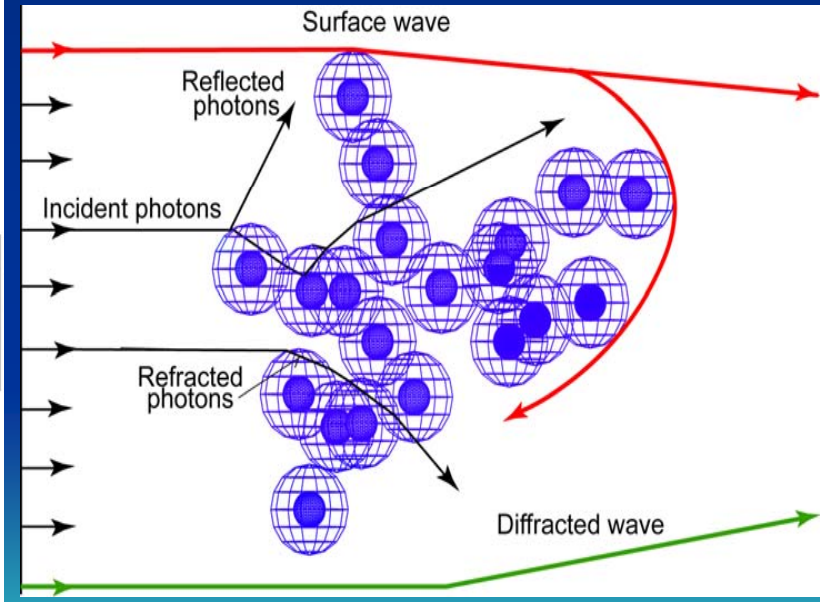

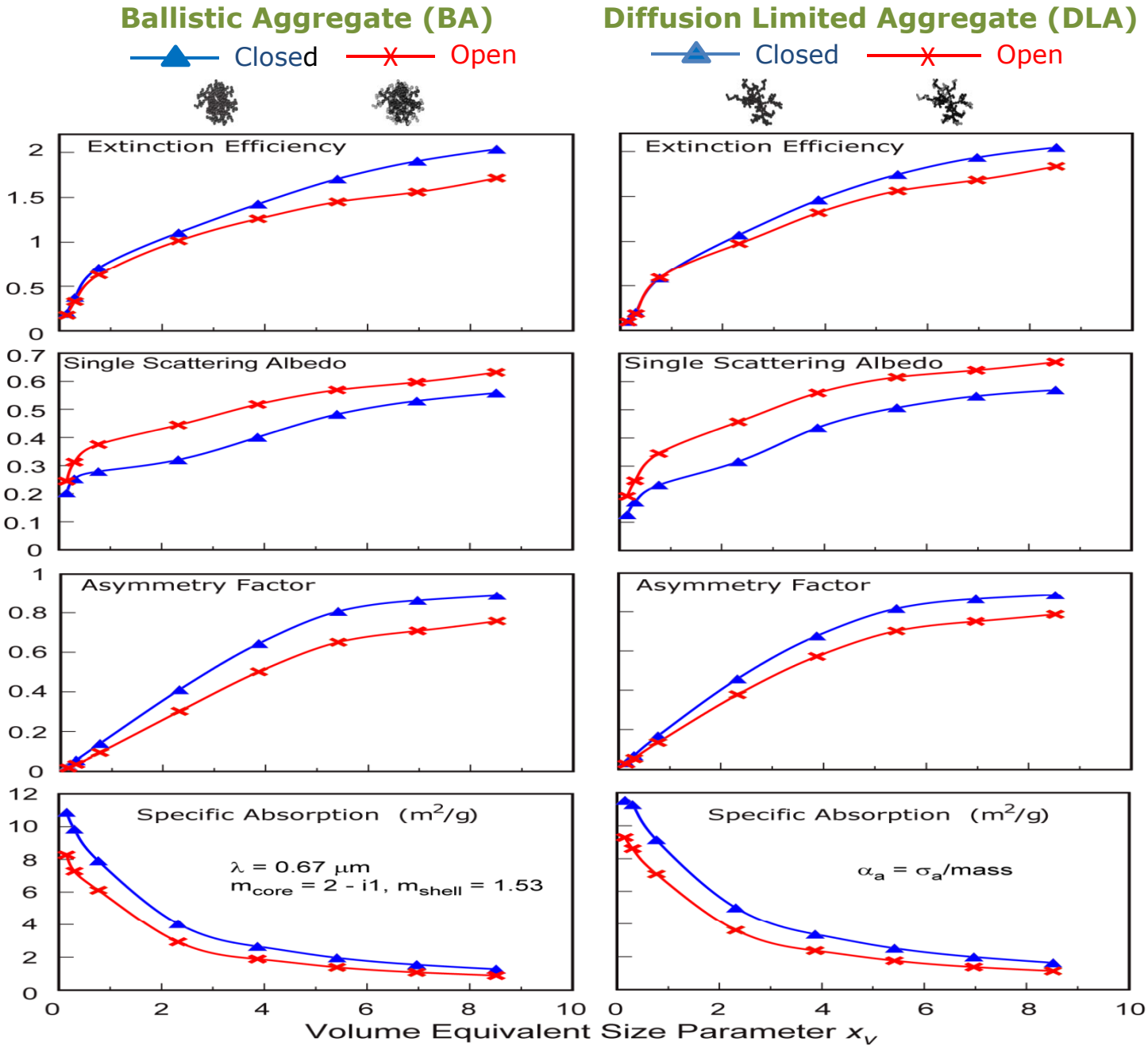

The single-scattering properties as a function of volume equivalent size parameter. 256 spheres were used to build BA and DLA based on stochastic procedures. Each building sphere in closed cell contains 90% soot core and 10% ammonium sulfate shell. In open cell, 70% are soot and 30% are sulfate such that volume and mass are the same in all cases. We show that closed cell cases have larger absorption and stronger forward scattering, as compared to open cell counterparts. Also, DLA absorbs more thar BA because of larger geometrical cross section.

Single-scattering co-albedo (the ratio of absorption and extinction coefficients) and snow albedo as a function of soot and dust equivalent radii for a snow grain (snowflake, see attached) of 50 μm in radius. Large differences in snow albedo are shown with absorbing aerosol contamination.

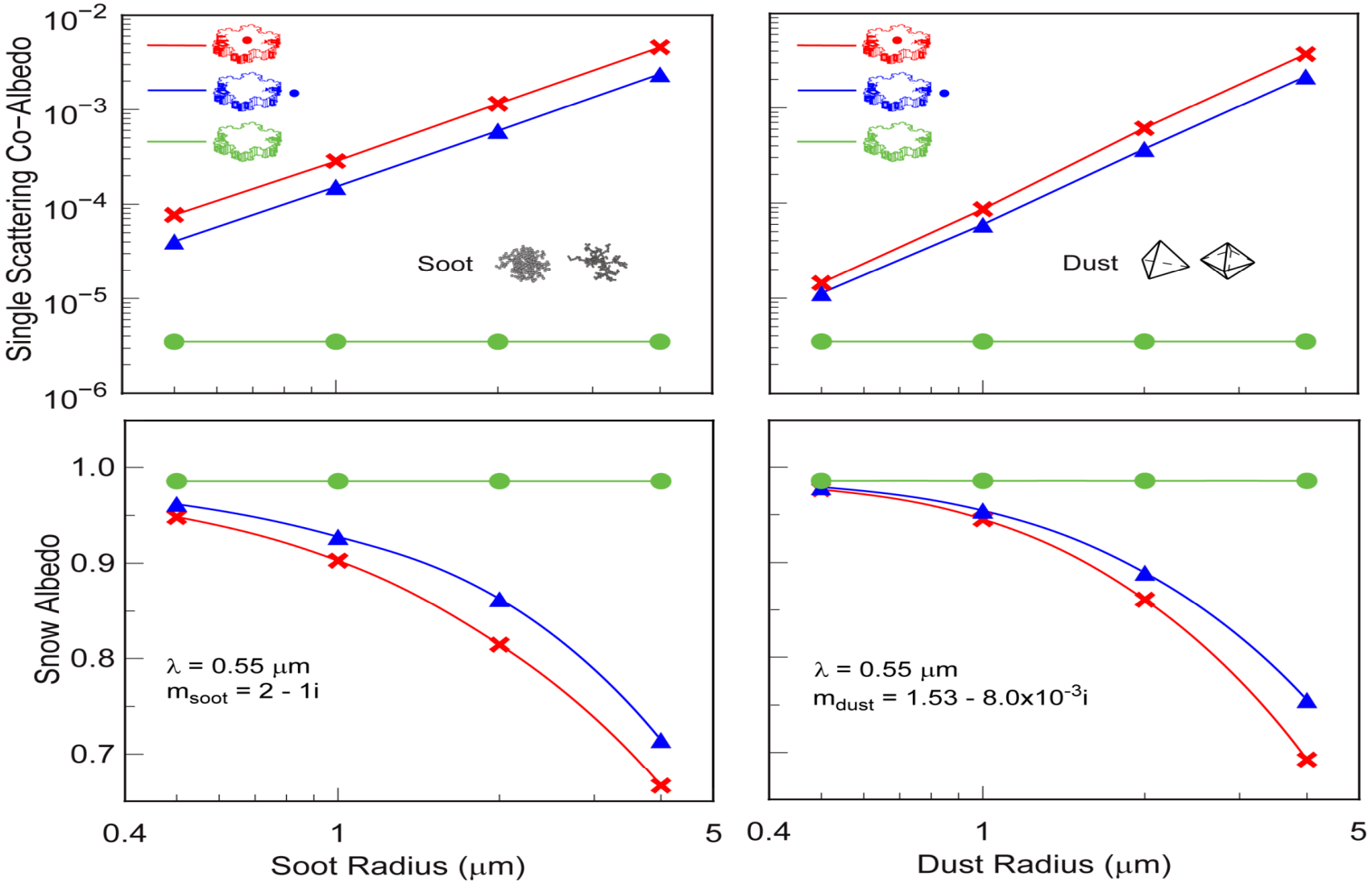

An Illustration of Mountains/Snow-Albedo Feedback due to Absorbing Aerosols

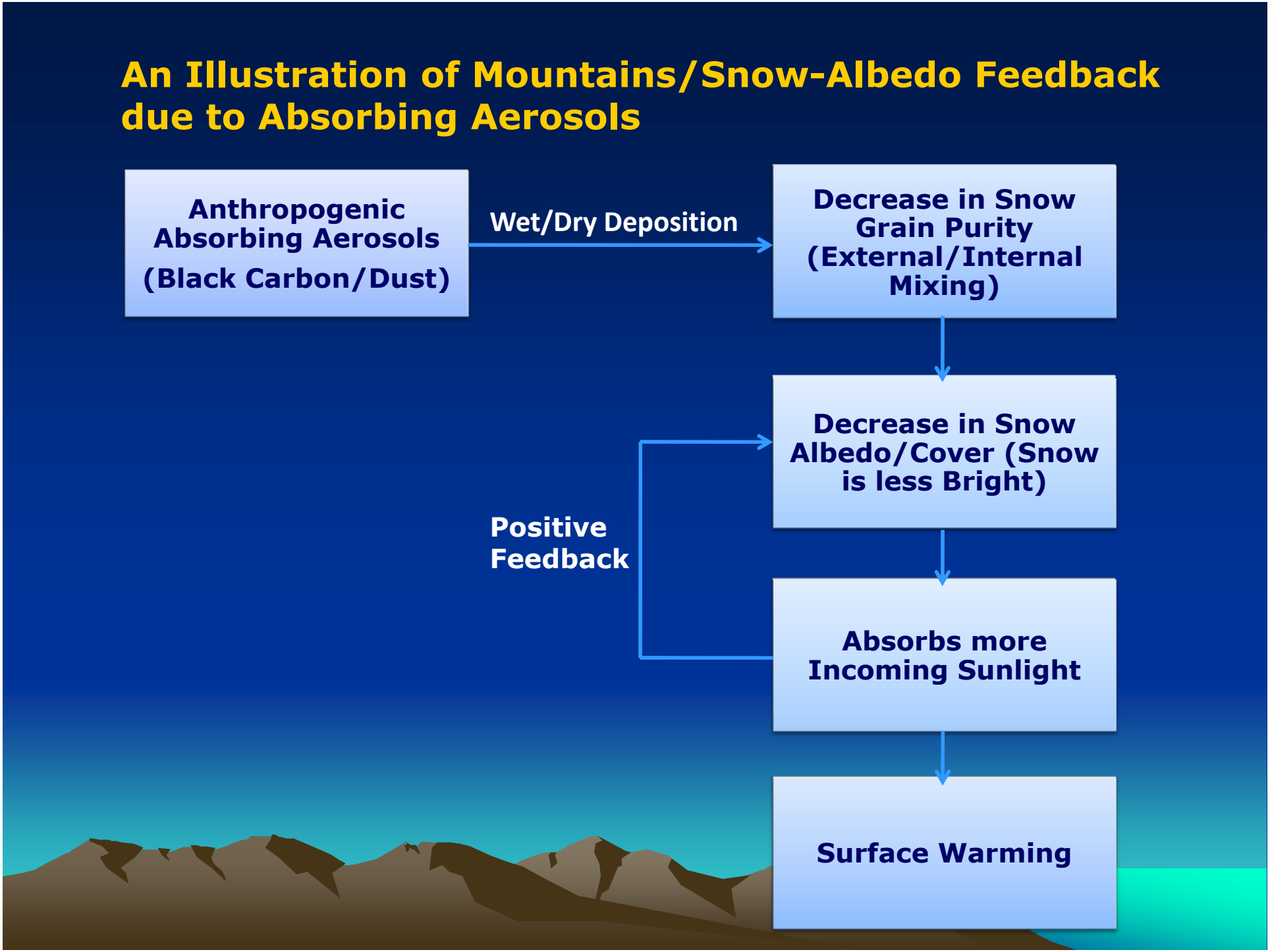

Summary: Radiation Parameterization for Climate Models

- We have identified a number of important and unsolved problems in radiative transfer and the needs for parameterization based on the first principle for climate models.
- Over a domain of 10x10-30x30 km^2 resolution, the 3D effects on intense topography can produce ~ 10-30 W/m^2 deviations from plane-parallel radiative transfer calculations commonly used in land surface models. We have illustrated that a regression-based parameterization for 3D direct, diffuse, and interactive solar fluxes is ready for testing in WRF-CLM (Leung et al. 2006).
- We have made fundamental advances in light absorption and scattering by aggregates (black carbon), but we need to comprehend the observed size, shape, and composition data to develop a useful parameterization for regional air-quality and climate models.